On-Cell Thickness Monitoring of Chalcogenide Alloy Layer using Spectral Interferometry, Raman spectroscopy, and Hybrid Machine Learning

Hyunwoo Ryoo*[a], Seul Ji Song[b], Min Ji Jeon[a], Juhyun Moon[b], JiHye Lee[a], ByungHyun Hwang[a], Jeongho Ahn[a], Yoon-jong Song[b], Hidong Kwak[a], Lior Neeman[c], Noga Meir[c], Jaehong Jang[d], Ik Hwan Kim[d], Hyunkyu Kim[d]

[a]DRAM Process Development Team MI, Samsung R&D Center, Hwaseong, Korea; [b]Advanced Technology Development Team, Samsung R&D Center, Hwaseong, Korea; [c]Nova Ltd, Rehovot, Israel; [d]Nova Measurement Instruments Korea Ltd, Gyeonggi-do, Korea.

ABSTRACT

The thickness of the chalcogenide ovonic threshold switching (OTS) layer is one of the most critical parameters for the switch-only memory (SOM) process control. Traditionally, the OTS thickness and composition were measured by XRF using the amounts of Ge, As, and Se. Still, XRF has a few limitations in delivering the required performance, especially for products with multilayer memory architecture. For these products, X-ray fluorescence (XRF) signals overlap and cannot be used to measure the thickness of each layer. In the current paper, we have studied three new alternative approaches for measurements of the OTS thickness on-cell: Spectral Interferometry, Raman spectroscopy, and Hybrid Machine Learning technique. The first method, Spectral interferometry with the Vertical Traveling Scatterometry approach (VTS), allowed OCD modeling of the top of the structure by blocking the complex underlayers and measuring only the top OTS thickness on all targets, including within the chip. The second method, Raman spectroscopy, demonstrated on-cell dimensional capabilities with an excellent correlation of the Ge-Se, As-Se, and Ge-Ge bonds of Raman active chalcogenide to TEM OTS thickness values. Finally, the third method used Raman parameters calibrated with TEM as a reference thickness for the ML solution using the VTS spectra on-cell. This ML method is fast, model-free, and requires minimal TEM samples for setup. All three methods have demonstrated capability for on-cell measurements and HVM process control.

Keywords: OTS thickness, Chalcogenide, Spectral Interferometry, Raman Spectroscopy, Hybrid Machine Learning

1. INTRODUCTION

1.1 Background

SOM (Selector Only Memory) products, which have recently emerged as next-generation memory semiconductors, use Chalcogenide-based OTS (Ovonic Threshold Switching) materials to enable memory and switching phenomena simultaneously. The advantage of OTS material is that it reduces leakage current and enables successful read/write operations. The thickness, temperature, and bandgap of GeAsSe compound OTS materials affect the threshold switching phenomenon, so OTS thickness measurements are critical during HVM **[1,2]**.

XRF (X-ray fluorescence) is currently the "tool of record" measuring OTS film thickness and composition in the semiconductor FAB. However, the signal strength of XRF decreases over time, requiring continuous calibration, which affects the accuracy of measurements. XRF is currently measuring the specially designed test site OS TEG (see Figure 1a), and its performance barely meets the process requirements for the thickness measurements. An additional limitation of the XRF is that for the SOM products with stack array OTS layers (see Figure 1b), the XRF signal overlaps between the upper OTS layer and the lower layer.

Metrology, Inspection, and Process Control XXXVIII, edited by Matthew J. Sendelbach, Nivea G. Schuch, Proc. of SPIE Vol. 12955, 129550G · © 2024 SPIE
0277-786X · doi: 10.1117/12.3012496

Therefore, new metrology methods are required to measure OTS thickness on multi-stack arrays. These methods should not be sensitive to the underlying structures to allow process control on-cell. The current study demonstrates that OTS thickness can be measured non-destructively on-cell using Spectral Interferometry, Raman spectroscopy, and hybrid ML technologies.

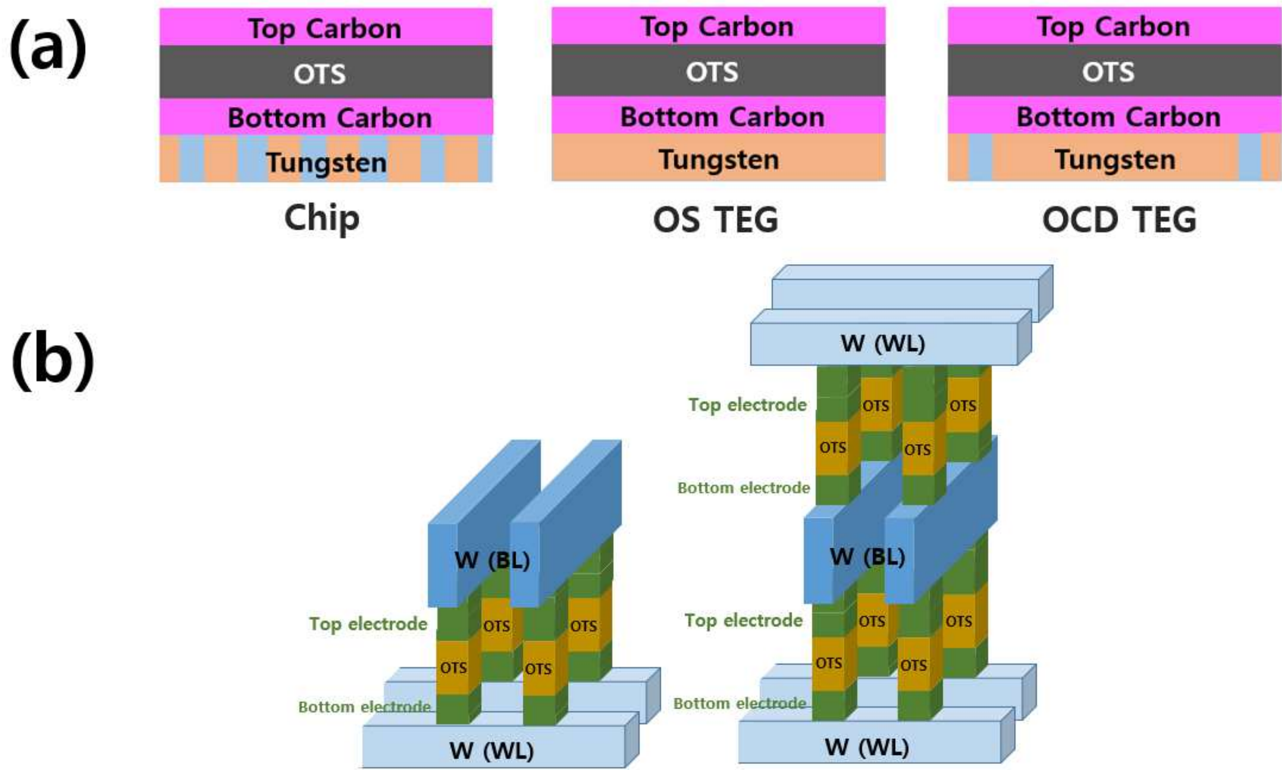

Figure 1. (a) The schematic presentation of the top part of the OTS structures measured, chip (on-cell), OS, and OCD TEG. **(b)** The architectural design of the single stack and bi-layer stack of OTS

1.2 Experimental details

Our study used three pattern wafers with split OTS thickness after the in-situ OTS deposition process **[Table 1].**

Table1. DOE information of the evaluation wafers used in this experiment

Slot	Stack structure	OTS thickness(Å)	Notation term
1	Top C/OTS/Bottom C	Low	S1
2	Top C/OTS/Bottom C	POR	S2
3	Top C/OTS/Bottom C	High	S3

We measured three measurement sites: OS and OCD TEG targets and an on-cell array in the chip (Figure 1a). All field wafer maps (119 points) were measured for each site. Figure 1a shows a schematic representation of the layer structure after OTS deposition, which will be the focus of our study on all measurement sites. Three blanket layers of Bottom Carbon,

OTS, and Top Carbon cover different W world line layer arrangements. In the chip and OCD targets, we have a line/space tungsten WL pattern, while in OS TEG WL, the layer is solid and not patterned. A comparison between the thickness measurements on these sites will allow us to determine if OS and OCD target sites can be used for process control of SOM manufacturing.

Figure 2a shows a typical spectrum of XRF measured in the OS TEG of three split OTS samples. Significant variations in XRF signal intensity for DOE wafers indicate good sensitivity to OTS thickness. Figure 2b shows the XRF peak deconvolution results of $Ge_{L\alpha}$, $As_{L\alpha}$, and $Se_{L\alpha}$. In particular, the elements of Ge, As, and Se exhibit the α signal of the L shell at 1.19, 1.29, and 1.39 keV, respectively. The correlation of XRF results with TEM reference (R^2=0.995) for three split OTS samples is shown in Figure 2c. Figure 2d presents the radial dependence of the OTS thickness measured by XRF. While XRF can simultaneously measure OTS's thickness and chemical composition, its long-term stability and precision are below HVM process monitoring requirements.

In addition, XRF penetrates deep into the sample (about a few microns). For the multilayer SOM products (shown in Figure 1b), XRF signals of the upper and lower OTS overlap and do not allow measurement of each layer's thickness.

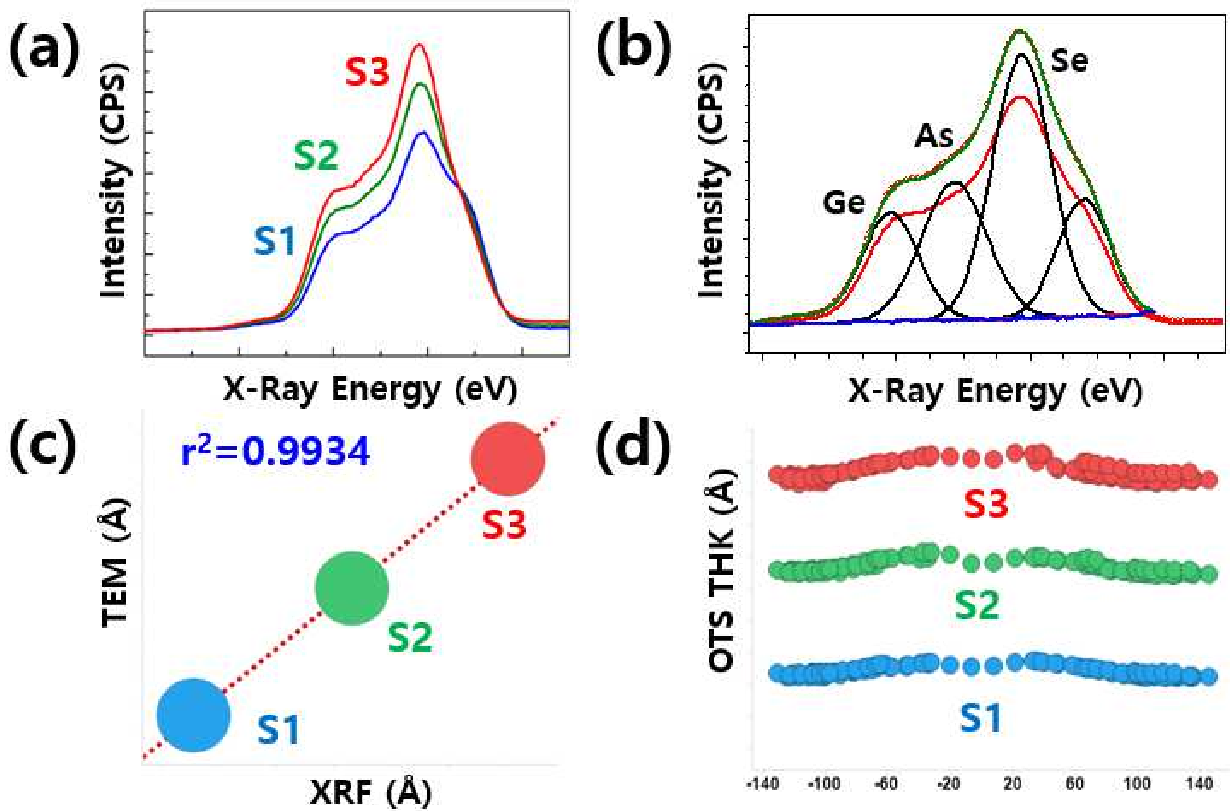

Figure 2. XRF measurement results on the OS TEG target. Typical XRF spectra of DOE wafers **(a)** and deconvolution of the XRF signal **(b)**, correlation of XRF OTS thickness to TEM **(c)**, and Radial plot of the OTS thickness **(d)**.

2. NEW STRATEGIES FOR OTS THICKNESS MEASUREMENT

Three methods, including Spectral Interferometry, Raman spectrometry, and hybrid ML, were studied to allow non-destructive monitoring of the OTS thickness on-cell (Figure 3). Spectral Interferometry combined with VTS technology enables the modeling of the top layers and filtering of the signals from complex bottom structures **[3].** Raman spectroscopy is the technology that can focus on Raman active materials, enabling measurement of OTS thickness and composition due to the sensitivity of the binding signal of the GeSeAs alloy. The hybrid ML solution uses raw spectra from spectral interferometry and OTS thickness from Raman measurement calibrated with TEM values.

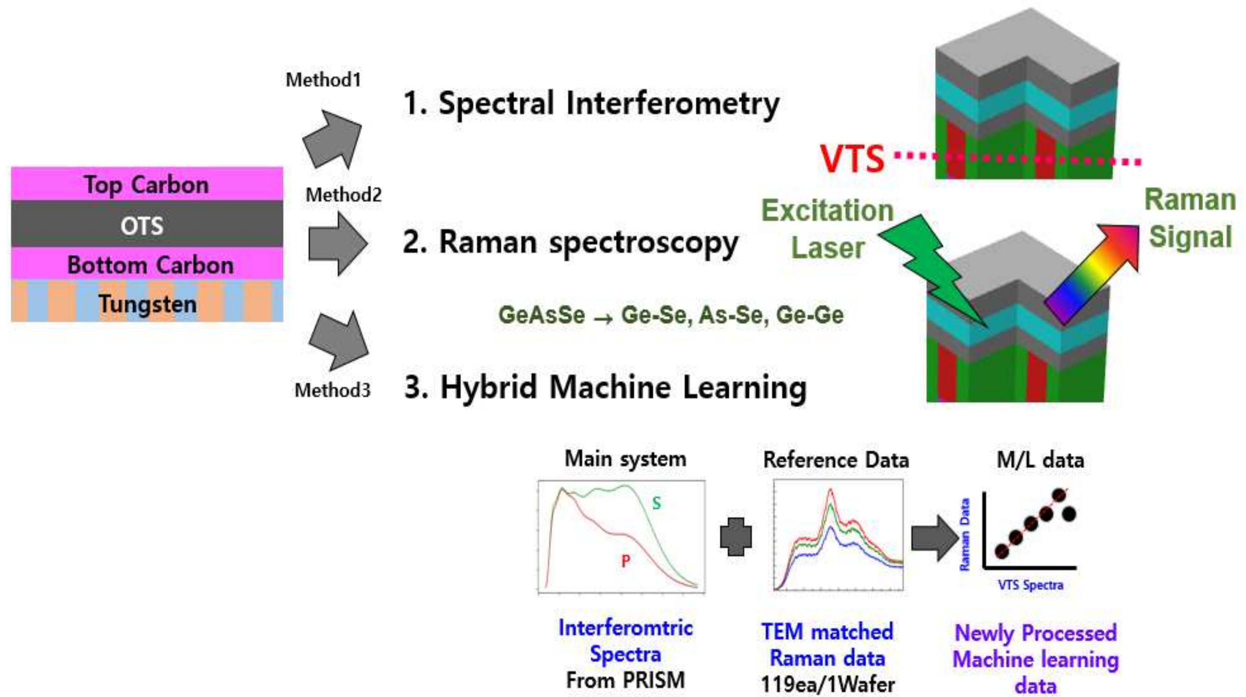

Figure 3. Three methods were studied to monitor the OTS thickness on-cell for SOM products: Spectral Interferometry, Raman spectroscopy, and hybrid ML.

2.1 Spectral Interferometry with VTS technology

Figure 4a shows the optical concept of the spectral interferometry equipment used in our study. The raw spectral signal obtained from the measurement is processed with unique VTS algorithms to generate a VTS signal less sensitive to the underlayers **[3].**

Figure 4b shows the OCD geometrical model used to measure the OTS thickness structure in the chip. Figure 4c shows the typical VTS spectra of OTS on-cell. The green ellipse highlights VTS peaks corresponding to the area of interest (top layers including OTS). The distance between VTS peaks can be used to calculate the thickness of the layers. The VTS filtering was performed to focus on the top layers and to eliminate the influence of the word line tungsten and all layers below.

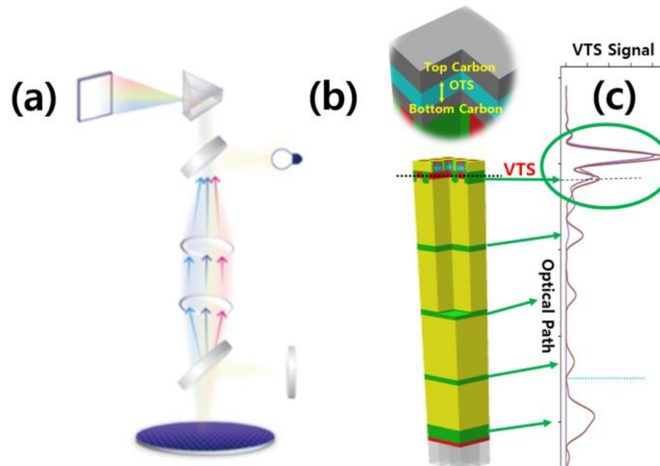

Figure 4. (a) Hardware scheme of spectral interferometry, **(b)** the OCD geometrical model used to measure OTS thickness structure in the chip, **(c)** Typical VTS signals. The oval marks the region corresponding to the cell's 'top carbon/OTS/bottom carbon' structure.

Figure 5 shows the spectra before and after VTS filtering obtained by measuring the three split samples used in this evaluation. The signal before VTS operation has several spectrum fringes, especially in the 200~500nm wavelength of A3 and A4; it can be seen that the spectrum simplifies after VTS by blocking the tungsten signal under the OTS. This ability of VTS to eliminate the signals of the underlayers improves the modeling and spectral fitting. It allows the measurement of top layer OTS thickness for all SOM products with more than one memory layer.

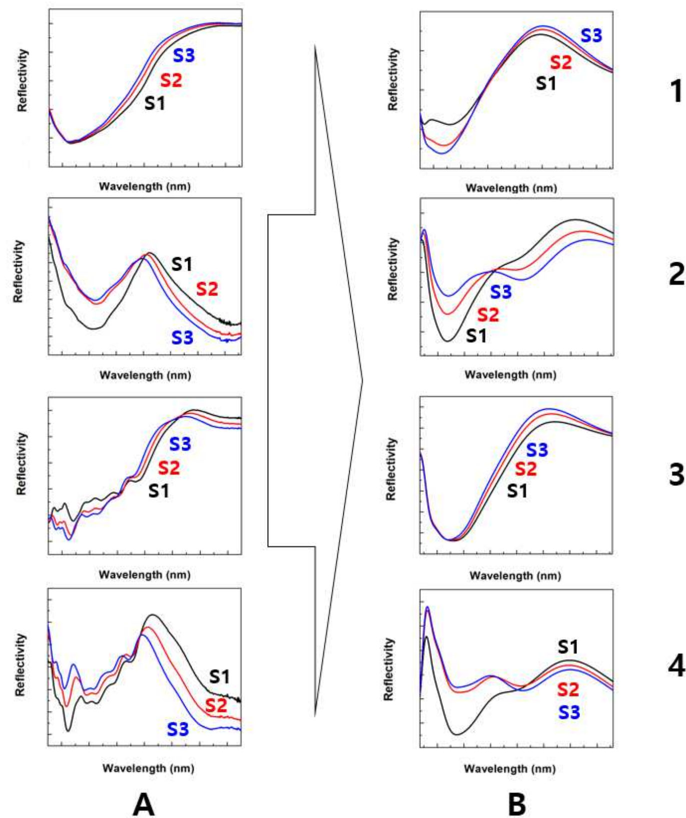

Figure 5. Raw spectral Interferometry signals **(A1-4)**, Spectral Interferometry signals after VTS filtering. **(B1-4)**

Figures 6a, b, and c show the spectral interferometry OTS thickness results obtained by modeling the VTS signal after filtering the underlayers on Cell, OCD, and OS TEG, respectively. We present a correlation to TEM, radial plot, and wafer map trends for each site for three DOE wafers studied. For all measurement sites, the correlation with TEM is high (R^2>0.995). For all measurement sites, there is a general trend of decreasing the OTS thickness from the center to the edges. However, on the very edge, OS TEG does not show the larger thickness trend observed in the OCD and cell. These results indicate the OTS thickness of OS TEG does not perfectly represent the thickness of the cell site.

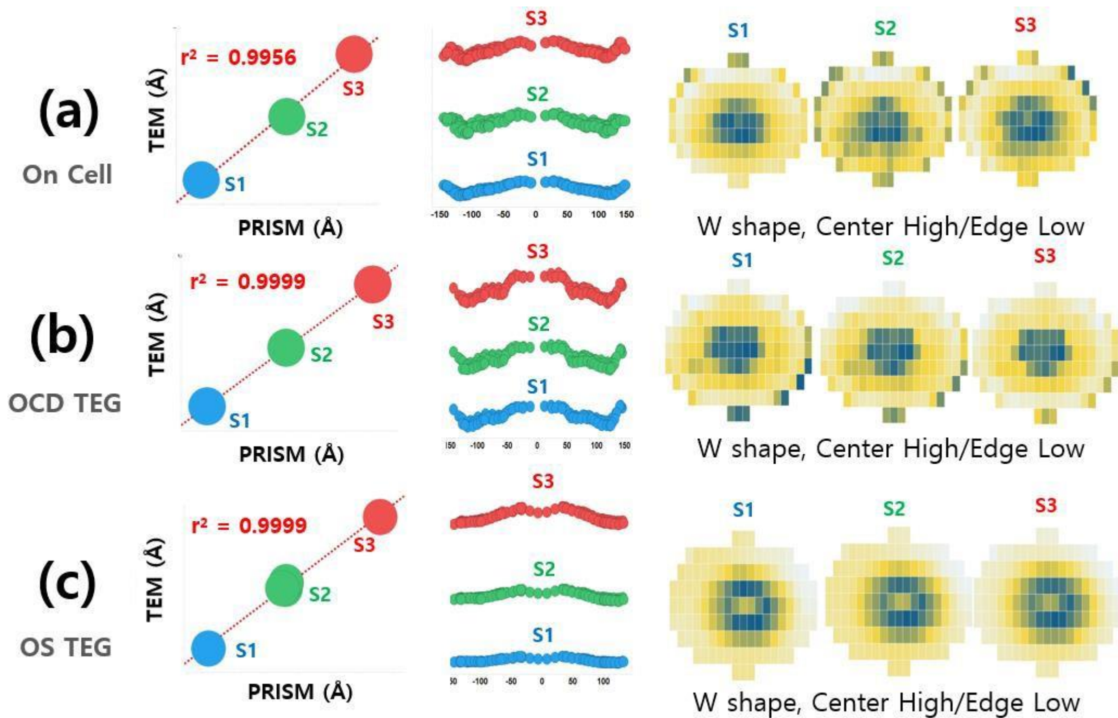

Figure 6. The OTS thickness results measured by spectral interferometry on cell (**a**), OCD (**b**), and OS TEG sites (**c**). Correlation to TEM, radial plots, and wafer maps are presented for all targets and all DOE wafers.

2.2 Raman Spectroscopy

Raman spectroscopy was the second metrology technique evaluated for the OTS thickness measurements on-cell for SOM products. The advantage of Raman spectroscopy is that it can measure Raman-sensitive materials in complex 3D structures and control the penetration depth by choosing the laser wavelength. In addition, the spot size of Raman is small enough to allow the required lateral resolution for the measurement of cell subarrays of the SOM products. In addition, Raman Spectroscopy enables the measurement of the composition and physical properties of the OTS material by analyzing Ge-Se, As-Se, and Ge-Ge chemical bonds. This paper focuses only on the area and intensity of deconvoluted Ge-Se, As-Se, and Ge-Ge peaks to measure the OTS thickness on-cell.

Figure 7a shows the typical Raman spectra of the OTS (amorphous GeAsSe alloy compound) DOE samples that demonstrate the sensitivity of the Raman signal to the changes in the OTS thickness. Figure 7b presents the spectra decomposition using the Lorentz model to separate Ge-Se, As-Se, and Ge-Ge binding signals at 190, 230, and 300cm^{-1}, respectively. In particular, the 190cm^{-1} Ge-Se bond signal corresponds to the corner-shared $Ge(Se_{1/2})_4$ tetrahedral unit, the 230cm^{-1} As-Se bond signal is a signal of the $AsSe_{3/2}$ pyramid unit **[4]**, while the 300cm^{-1} Ge-Ge bond is of an ethanlike (ETH) structure with a bond between broken Ge-Se_2 units **[5]**. Therefore, these bonding signals of GeAsSe can provide crucial information on the concentration and physical properties of the chalcogenide material of SOM products, as demonstrated in studies of OTS changes with temperature **[6]** or damage **[7]**. In addition, Raman signal parameters related to the binding energy of OTS are essential for trap density research to analyze the OTS mechanism **[8]**.

Figure 7c explains how Raman signals were used to measure the thickness of the OTS on-cell site in this study. The peak area and intensity of the three deconvoluted signals corresponding to Ge-Se, As-Se, and Ge-Ge bonds showed an excellent correlation to TEM. From this linear correlation, we can calculate the OTS thickness for all Raman measurements and use any of the six Raman parameters studied to monitor the OTS film.

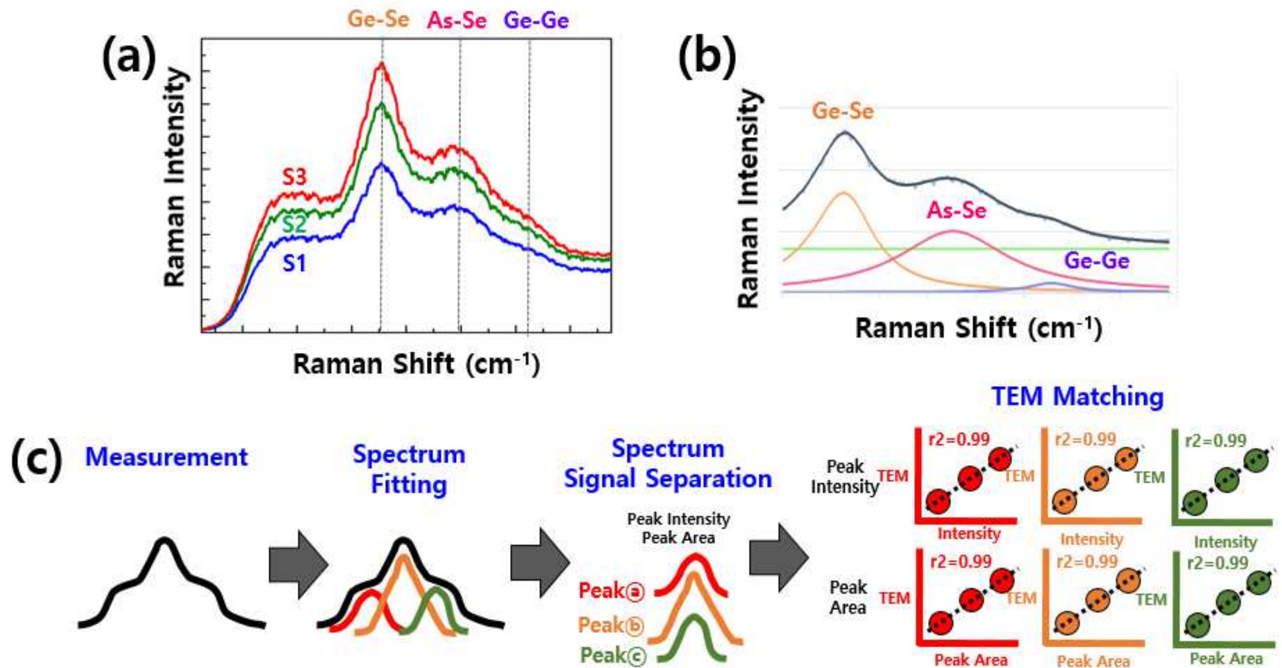

Figure 7. (a) Typical Raman spectra of split samples with OTS thickness **(b)** Result of deconvolution of Raman signal of OTS layer **(c)** Technical concept explaining how Raman signals can be used to measure the thickness of the on-cell site of OTS

Figure 8 shows the OTS thickness results measured by Raman spectroscopy on-cell by converting the peak area and intensity of the Ge-Se, As-Se, and Ge-Ge binding signals into the thickness from TEM correlation. Figure 8a shows the peak area and intensity correlations with TEM for all three bonds (Ge-Se, As-Se, and Ge-Ge) used to calculate the thickness. For all Raman parameters (Ge-Se area, As-Se area, Ge-Ge area, Ge-Se intensity, As-Se intensity, and Ge- Ge intensity), there is a high correlation to TEM with R^2 above 0.99 when matched with TEM. This high correlation shows that there is a potential to measure the OTS thickness on-cell with the Raman signal values converted to TEM. We have used radial trends (Figure 8b) and wafer maps (Figure 8c) of the Raman OTS thickness based on different parameters to compare the best Raman parameters. Radial trends for the OTS thickness calculated for all Raman parameters show the expected thickness decrease from the center to the edge, with a slight increase at the extreme edge (Figure 8b). However, there are larger spreads on the radial dependence data for the thickness calculated from the Ge-Ge peak area and intensity than from the Ge-Se and As-Se.

Similar behavior can also be seen by comparing the wafer maps of the OTS thickness calculated from 6 Raman parameters in Figure 8c. The OTS thickness wafer map calculated from the Ge-Ge signal's parameters differs from other wafer maps: we can barely see the expected radial trends because of significant non-uniformity. This non-uniformity is probably due to the smaller intensity and peak area of the Ge-Ge signal compared to other Raman signals, resulting in a smaller signal-to-noise SNR ratio. Wafer maps of the Ge-Se and As-Se Raman Signals area and intensities have expected radial trends, similar to the SI wafer maps (see Figure 6a). Our results show that Raman spectroscopy signals can be used to monitor the OTS thickness.

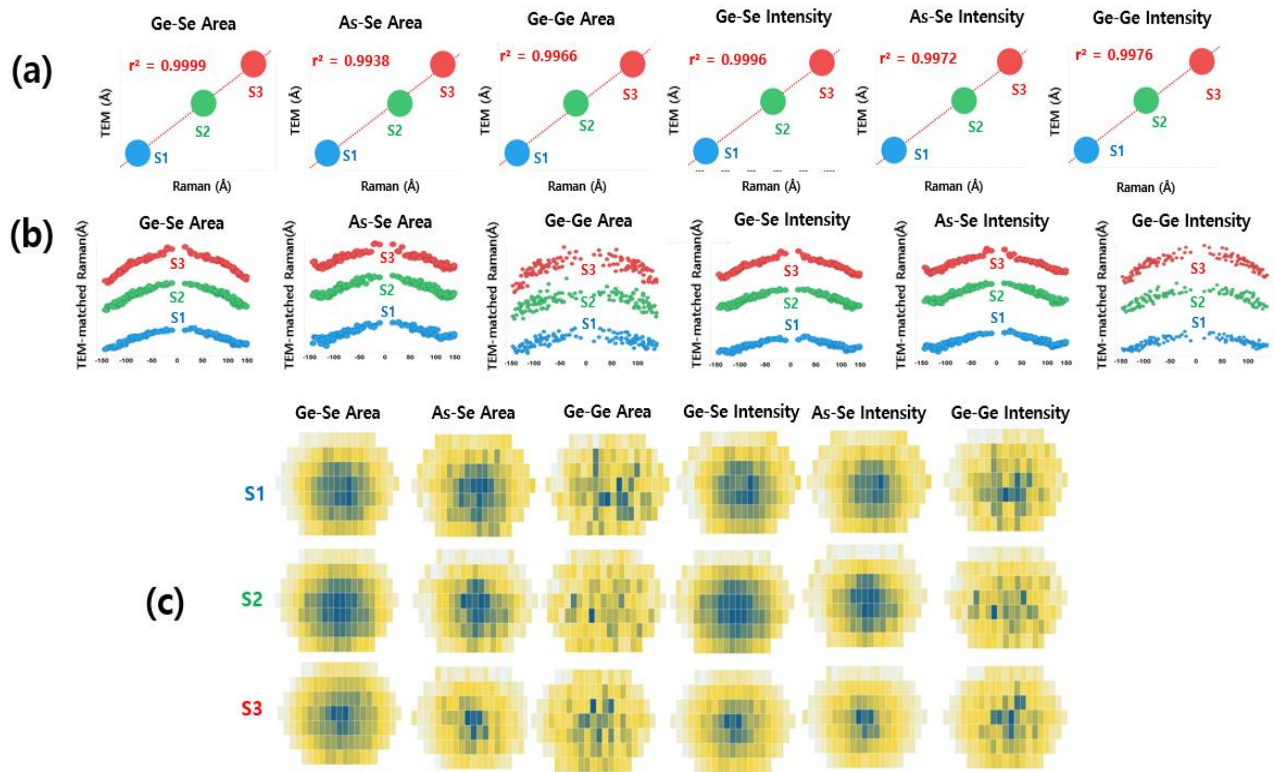

Figure 8. **(a)** Correlation between the Raman signals (Ge-Se area, As-Se area, Ge-Ge area, Ge-Se intensity, As-Se intensity, and Ge-Ge intensity) and TEM OTS thickness. **(b)** Radial dependences and **(c)** wafer maps of the OTS thickness from all six Raman signal parameters converted to TEM values.

2.3 Hybrid Machine Learning

This session presents the third metrology technique for the OTS thickness measurement on-cell - the hybrid machine learning (ML) technology. Hybrid ML technology concept is described in Figure 9; it is the interferometric signal processed with VTS as an input for ML and OTS thickness calculated from Raman signal calibrated by TEM as a reference for ML training.

Figure 10 shows the validation of Hybrid ML solutions created using all Raman parameters (Ge- Se area, As-Se area, Ge-Ge area, Ge-Se intensity, As-Se intensity, and Ge-Ge intensity) calibrated to the TEM values. Validation was done using the test on train validation method (Figure 10a) and die level accuracy test method (Figure 10b). Validation results (R^2 and standard deviation) can be used to compare all Raman parameters' performance for measuring the OTS thickness. ML solutions based on the Ge-Ge Raman signal (area and intensity) for both validation types show the worst performance compared to ML based on other parameters, as expected based on earlier observation (see Figure 8). The peak intensity parameter shows higher R^2 and lower standard deviation than the Raman peak area. Ge-Se signal-based ML solutions are slightly better than As-Se. Overall, the Ge-Se intensity parameter has the highest R^2 and the lowest standard deviation, so it can be considered the most suitable candidate for the Hybrid ML on-cell OTS thickness monitoring.

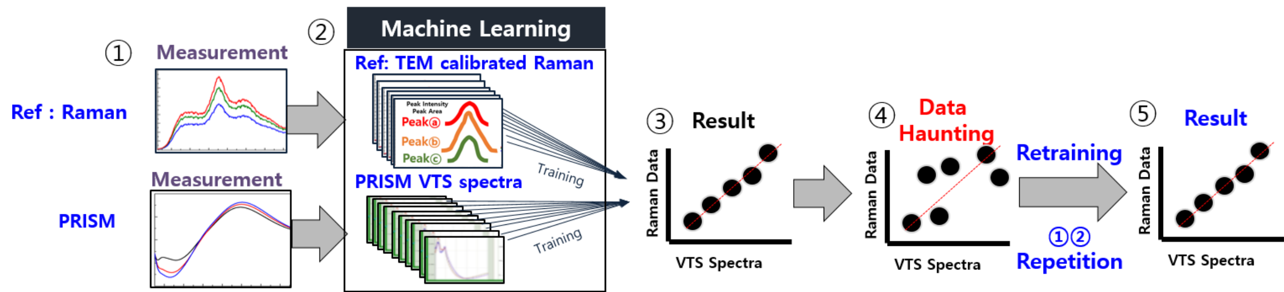

Figure 9. Scheme explaining the concept of hybrid ML technology used for measurements of the on-cell OTS thickness.

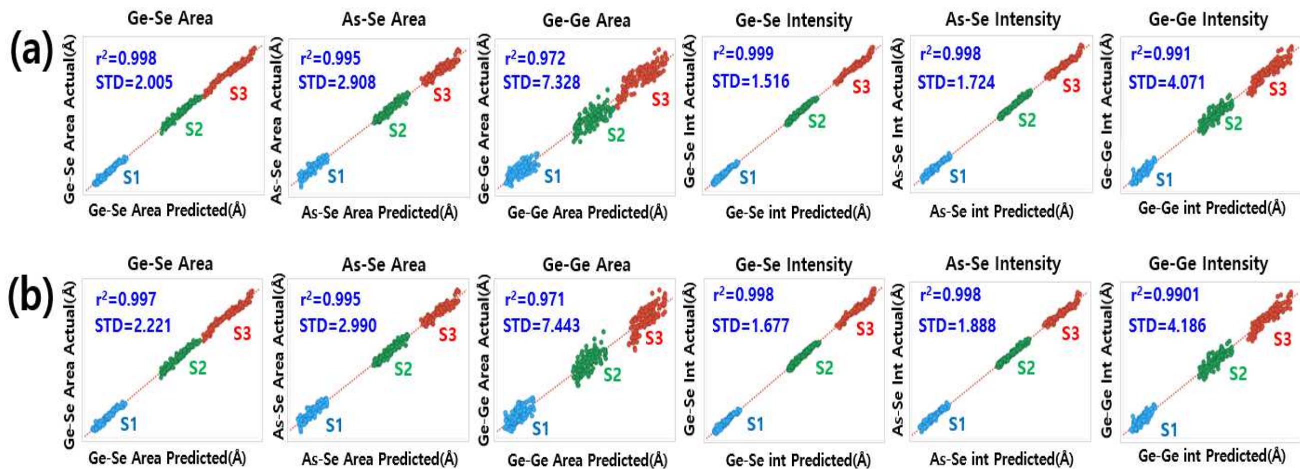

Figure 10. Correlations between the predicted ML results and reference data (Raman signals calibrated with TEM): Using the test on train validation method **(a)** and the cross-validation die level accuracy method **(b).** STD is 1sigma in A.

Additional validation of the Hybrid ML performance is done by analysis of the radial trends and wafer maps (See Figure 11). Hybrid ML solutions based on all Raman parameters, besides the Ge-Ge-based, show the expected DOE split and radial behavior with the expected decrease of the OTS thickness from the center to the edge.

We can highlight a few advantages of the proposed hybrid ML approach based on VTS signals trained on Raman and calibrated by the TEM. First, it eliminates the need for modeling while utilizing the best techniques, including the VTS filtering of underlayers and Raman focusing on Raman-sensitive materials and depth penetration control. Second, it eliminates the need for multiple expensive and destructive TEM references and DOE wafers, making robust training more accessible and straightforward. In addition, the Hybrid ML solutions based on multiple Raman parameters can be used for cross-checking when verifying the consistency of ML data. In addition, the six types of Raman signal parameters used in this study are the thickness values of OTS on-cell converted to TEM values. Additionally, since both Spectral interferometry and Raman spectrometer are implemented in high-volume manufacturing (HVM) Fab if there is a data consistency issue or process change, Hybrid ML can be immediately retrained by re-measuring the sample by Raman spectrometry and recalculating the reference data.

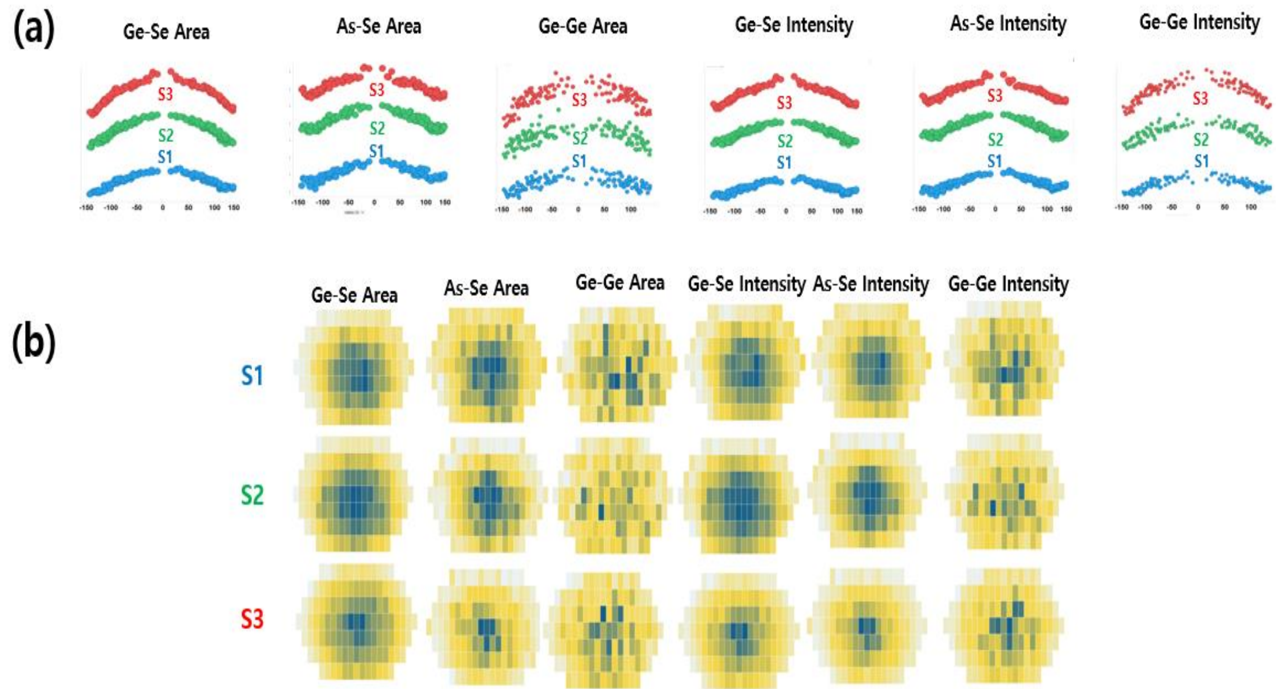

Figure 11. Radial plots **(a)** and wafer maps **(b)** of the OTS thickness measured by Hybrid ML method.

3. SUMMARY AND CONCLUSION

Spectral Interferometry, Raman spectroscopy, and hybrid ML technologies were successfully evaluated for on-cell OTS thickness monitoring.

OCD modeling of Spectral Interferometry with VTS technology can measure OTS thickness on-cell by blocking the word line tungsten and underlayer's signals and extracting only signals of the top OTS layer. In particular, the interferometric signal after the VTS operation becomes much more straightforward than the raw signal before the VTS operation, making OCD modeling and spectrum fitting easier and improving data consistency.

In addition, Raman spectroscopy technology focusing on the Raman-sensitive OTS layer demonstrated dimensional capabilities by showing an excellent correlation to the on-cell TEM thickness of the OTS layer. Deconvoluted Ge-Se and As-Se peak area and intensity were qualified to measure the thickness directly, in addition to composition and other essential material properties, such as trap energy.

Lastly, Hybrid ML technology was implemented for on-cell OTS thickness measurements. The proposed Hybrid ML approach utilizes the VTS-processed interferometric signals, with the Raman signal parameters calibrated by TEM values as a reference. Among the advantages of this method is that it increases robustness and data reliability by using multiple references instead of expensive and destructive TEMs. Furthermore, when the process changes, fab engineers can improve data consistency by re-measuring Raman spectroscopy, recalculating reference data, and retraining Hybrid ML solutions.

All three proposed methods - Spectral Interferometry, Raman spectroscopy, and Hybrid ML technologies - are non-destructive, fast, have small spot sizes, and can measure top OTS thickness on-cell and for all multilayer SOM products

ACKNOWLEDGEMENTS

The authors thank Dr. YunJung Jee and Dr. Sang Hyun Han for their help in preparing this paper.

REFERENCES

[1] A. Velea, K. Opsomer, W. Devulder, J. Dumortier, J. Fan, C. Detavernier, M. Jurczak, and B. Govorreanu, "Te-based chalcogenide materials for selector applications," Sci. Rep. 7, 8013 (2017). DOI:10.1038/s41598-017-08251-z

[2] M. Nardone, V. G. Karpov, D. C. S. Jackson, and I. V. Karpov, "A unified model of nucleation switching," Appl.Phys.Lett. 94, 103509 (2009). https://doi.org/10.1063/1.3100779

[3] D. Schmidt, C. Durfee, S. Pancharatnam, M. Medikonda, A. Greene, J. Frougier, A. Cepler, G. Belkin, D. Shafir, R. Koret, R. Shainman, I. Turvets, and S. Wolfling, "OCD enhanced: Implementation and Validation of Spectral Interferometry for Nanosheet Inner Spacer Indentation," Proc. SPIE 11611, 11611U (2021). doi: 10.1117/12.2582364

[4] K. Shportko, L. Revutska, O. Paiuk, J. Baran, A. Stronski, A. Gubanova, and E. Venger, "Compositional dependencies in the vibrational properties of amorphous Ge-As-Se and Ge-Sb-Te chalcogenide alloys studied by Raman spectroscopy," Opt. Mater. 73, 489-496 (2017). https://doi.org/10.1016/j.optmat.2017.08.042

[5] K. Jackson, A. Briley, S. Grossman, D. V. Porezag, and M. R. Pederson, "Raman-active modes of a-GeSe2 and a-GeS2: A first-principles study," Phys. Rev. B 60, R14985-R14989 (1999). https://doi.org/10.1103/ PhysRevB.60.R14985

[6] D. Sahoo, P. Priyadashini, A. Aparimita, D. Alagarasan, R. Ganesan, S. Varadharajaperumai, and R. Naik, "Role of annealing temperature on optimizing the linear and nonlinear optical properties of As40Se50Ge10 films," RCS.Adv 10, 26675-26685 (2020). https://doi.org/10.1039/D0RA04763E

[7] S. Clima, D. Garbin, W. Devulder, J. Keukelier, K. Opsomer, I. Goux, G. S. Kar, and G. Pourtois, "Material relaxation in chalcogenide OTS SELECTOR materials," Microelectronic Engineering 215, 110996 (2019). https://doi.org/10.1016/j.mee.2019.110996

[8] M. Lee, S. Lee, M. Kim, S. Lee, C. Won, T. Kim, C. Kwon, K. Yoon, J. Lee, H. Kim, and T. Lee, "$Ge_{1-x}S_x$ chalcogenide alloys for OTS applications using magnetron sputtering," Journal of Alloys and Compounds" 930, 167409 (2023). https://doi.org/10.1016/j.jallcom.2022.167409